BIOCHEMISTRY

 Volume 44, Number 38 September 27, 2005

New Concepts

Bench Meets Bedside: A 10-Year-Old Girl and Amino Acid Residue Glycine 75 of the Facilitative Glucose Transporter GLUT1

Jörg Klepper,*,‡ Alexis Salas-Burgos,§ Elena Gertsen,‡ and Jorge Fischbarg§

Department of Pediatrics and Pediatric Neurology, University of Essen, Hufelandstrasse 55, D-45122 Essen, Germany, and Department of Physiology and Cellular Biophysics and Ophthalmology, Columbia University, New York, New York 10027

Received June 6, 2005; Revised Manuscript Received July 11, 2005

ABSTRACT: In 2000, amino acid residue G75 of the facilitative glucose transporter GLUT1 was identified by mutagenesis as being essential for transport function [Olsowski, A., et al. (2000) *Biochemistry 39*, 2469−74]. In 2002, we identified a heterozygous missense mutation substituting glycine at residue 75 for tryptophan in a 10-year-old girl with intractable seizures and low glucose concentrations in the cerebrospinal fluid indicative of GLUT1 deficiency. Glucose uptake into erythrocytes of the patient was 36% of controls, and GLUT1-specific immunoreactivity was normal, indicating a functional GLUT1 defect. In silico three-dimensional modeling of the G75W mutant provided a smaller gyration radius for transmembrane segment 2 as the potential pathogenic mechanism in this patient. This case illustrates a GLUT1 mutation characterized in vitro and later confirmed by disease itself and highlights the potential of basic science and clinical medicine to collaborate for the benefit of patients.

Basic scientists and clinicians share a common interest: they want to elucidate disease mechanisms and thus contribute to the progress of science for the benefit of patients. The approaches they use often differ, and increasing subspecialities obstruct the dialogue between disciplines. However, the exchange of ideas and the coordination of research efforts are essential in achieving optimal results. In 2000, Olsowski et al. (*1*) reported that the amino acid residue glycine at position 75 (G75) of the facilitative glucose transporter GLUT1[1] is essential for glucose transport function. Two years later, we identified a heterozygous mutation substituting tryptophan for glycine at position 75 in a 10-year-old girl with an epileptic encephalopathy and low glucose concentrations in the cerebrospinal fluid (CSF). These features are characteristic of GLUT1 deficiency syndrome, a clinical entity resulting from impaired GLUT1-mediated glucose transport across the blood−brain barrier (*2*). In an collaborative effort, we unraveled a possible structural basis for the disease mechanism in this child.

BACKGROUND

The Facilitative Glucose Transporter GLUT1. As D-glucose is the essential substrate for energy metabolism, scientists have long been interested in glucose transport. In human brain, the transfer of glucose across the blood−brain barrier is exclusively mediated by the facilitative glucose

* To whom correspondence should be addressed: Department of Pediatrics and Pediatric Neurology, University of Essen, Hufelandstrasse 55, D-45122 Essen, Germany. Phone: +49 201 723 2356. Fax: +49 201 723 2333. E-mail: joerg.klepper@uni-essen.de.

‡ University of Essen.

§ Columbia University.

[1] Abbreviations: GLUT1, facilitated glucose transporter protein type 1; MCT1, monocarboxylate transporter type 1; CSF, cerebrospinal fluid; 3-OMG, 3-*O*-methyl-D-glucose; PCR, polymerase chain reaction; MDS, molecular dynamics simulation; rmsd, root-mean-square deviation; rmsf, root-mean-square fluctuation.

10.1021/bi051079t CCC: $30.25
Published on Web 09/01/2005

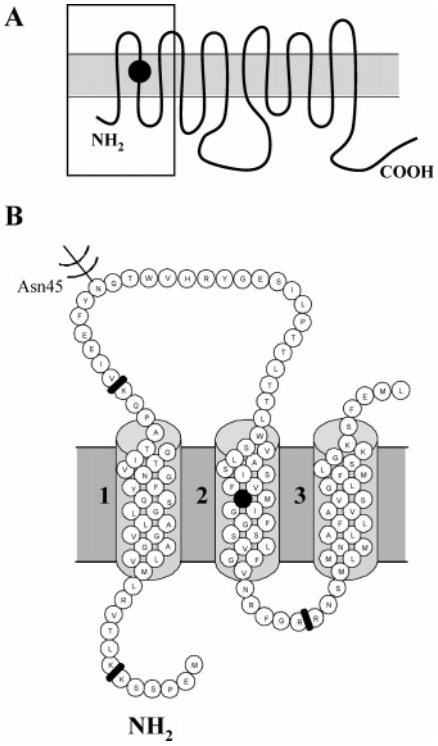

FIGURE 1: (A) Conformational model for the orientation of GLUT1 in the membrane as proposed by Mueckler et al. (*4*) with the G75W mutation (●) and intron−exon boundaries (−). (B) Detailed section of the amino terminus and transmembrane segments 1−3. The G75W mutation is shown in transmembrane segment 2 (●).

transporter protein GLUT1 (*3*). GLUT1, encoded by a single gene located on the short arm of chromosome 1 (1p35-31.3), is a transmembrane glycoprotein consisting of 492 amino acids with a molecular mass of 54 kDa and a high affinity for D-glucose (*4*). It carries the characteristic signatures of sugar/polyol transporters: (i) the presence of 12 membrane-spanning transmembrane segments, (ii) seven conserved glycine residues in the transmembrane segments, (iii) several basic and acidic residues at the intracellular surface of the proteins, (iv) two conserved tryptophan residues, and (v) two conserved tyrosine residues (*5*). A 12-transmembrane-spanning α-helical model for the Glut proteins proposed by Mueckler et al. (*4*) in 1985 places the amino and carboxy termini intracellularly with every consecutive transmembrane segment crossing the membrane in alternating directions (Figure 1A). This model was supported by subsequent mutagenesis (*6*). Mutational and affinity labeling studies as well as site-directed mutagenesis have indicated key residues and regions involved in sugar and inhibitor binding (*7*−*9*). According to the distribution of hydrophilic and hydrophobic amino acid residues, transmembrane segments 3, 5, 7, 8, and 11 are amphipathic segments and may form an aqueous pathway that the glucose molecule could traverse through the cell membrane (*10*). The recent advent of the 1SUK model for Glut1 derived on the basis of homology (*11*) has placed all these prior studies on a much more solid footing, as the 1SUK structure confirms them, and accounts for all mutagenesis and biochemistry evidence.

D-Galactose, D-mannose, dehydroascorbic acid, H_2O, and glycopeptides (*7*, *12*) have been identified as additional GLUT1 substrates. GLUT1 is a high-affinity glucose transporter, and a K_m of 2−5 mmol ensures function close to V_{max} under physiological conditions where blood glucose amounts

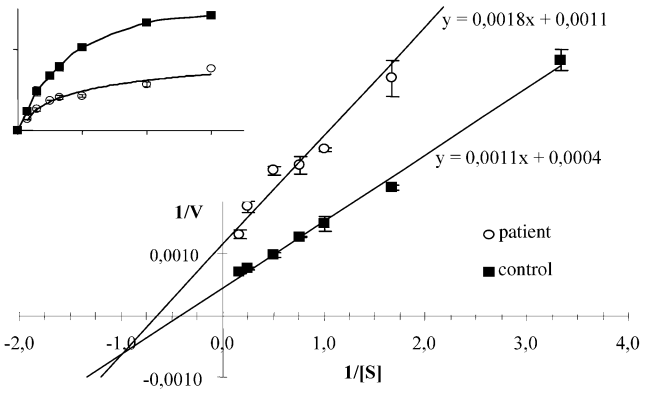

FIGURE 2: Kinetic analysis of uptake of 3-OMG by erythrocytes (four determinations per data point). Double-reciprocal plot of the substrate dependence for 3OMG transport into erythrocytes of the patient and a parental control. Uptake was assessed over 15 s in the presence of concentrations of 3-OMG ranging from 0.3 to 5 mmol/L. The inset shows the same 3-OMG uptake data vs [3OMG] (mmol/L). *Y* axis units are femtomoles per second per 10^6 RBC.

are approximately 5 mmol. Kinetic analysis of Glut1-mediated transport in human erythrocytes supports a simple alternating conformational model for facilitative transport (*13*, *14*) with an allosteric pore (*15*) endowed with a movable gate (*16*) such that the substrate induces conformational changes involving the gate and the rest of the protein.

The Disease. In 1991, De Vivo et al. (*17*) recognized a novel disease caused by impaired GLUT1-mediated glucose transport across the blood−brain barrier and into brain cells. This entity is now recognized as GLUT1 deficiency syndrome. The biochemical hallmark of the disease is a low CSF glucose concentration (hypoglycorrhachia); this results in an epileptic encephalopathy with early-onset seizures, variable developmental delay, and a complex movement disorder. Currently, the entity has been identified in ∼100 patients worldwide. The GLUT1 defect can be confirmed by quantitative and functional studies of the GLUT1 protein in erythrocytes. Several private heterozygous mutations in the GLUT1 gene (1p35-31.3) and autosomal-dominant transmission have been reported (for reviews see refs *2*, *18*, and *19*). Most importantly, this childhood encephalopathy can be treated effectively by means of a ketogenic diet. This high-fat, low-carbohydrate diet mimics the metabolic state of fasting providing ketone bodies that serve as an alternative fuel to the brain, thus bypassing the impaired glucose transport in these patients.

MATERIAL, METHODS, AND RESULTS

The Patient. This 10-year-old Austrian girl developed several episodes with unconsciousness, cyanosis, and peculiar eye movements at the age of 8 months. A full medical and metabolic workup, including neuroimaging, was uninformative except for a subaortical ventricular septal defect unrelated to the symptoms. At age 14 months, she developed secondary generalized seizures. At this time, significant psychomotor developmental delay was apparent: the child walked unassisted at 17 months with a spastic, ataxic gait, and used first words at 3.5 years of age. Seizures were unresponsive to anticonvulsant medication, but improved on sugar intake. At age 5.4 years, a lumbar puncture showed a low glucose concentration in the cerebrospinal fluid (CSF) in the setting of normoglycemia (blood glucose, 4.94 mmol/L; CSF

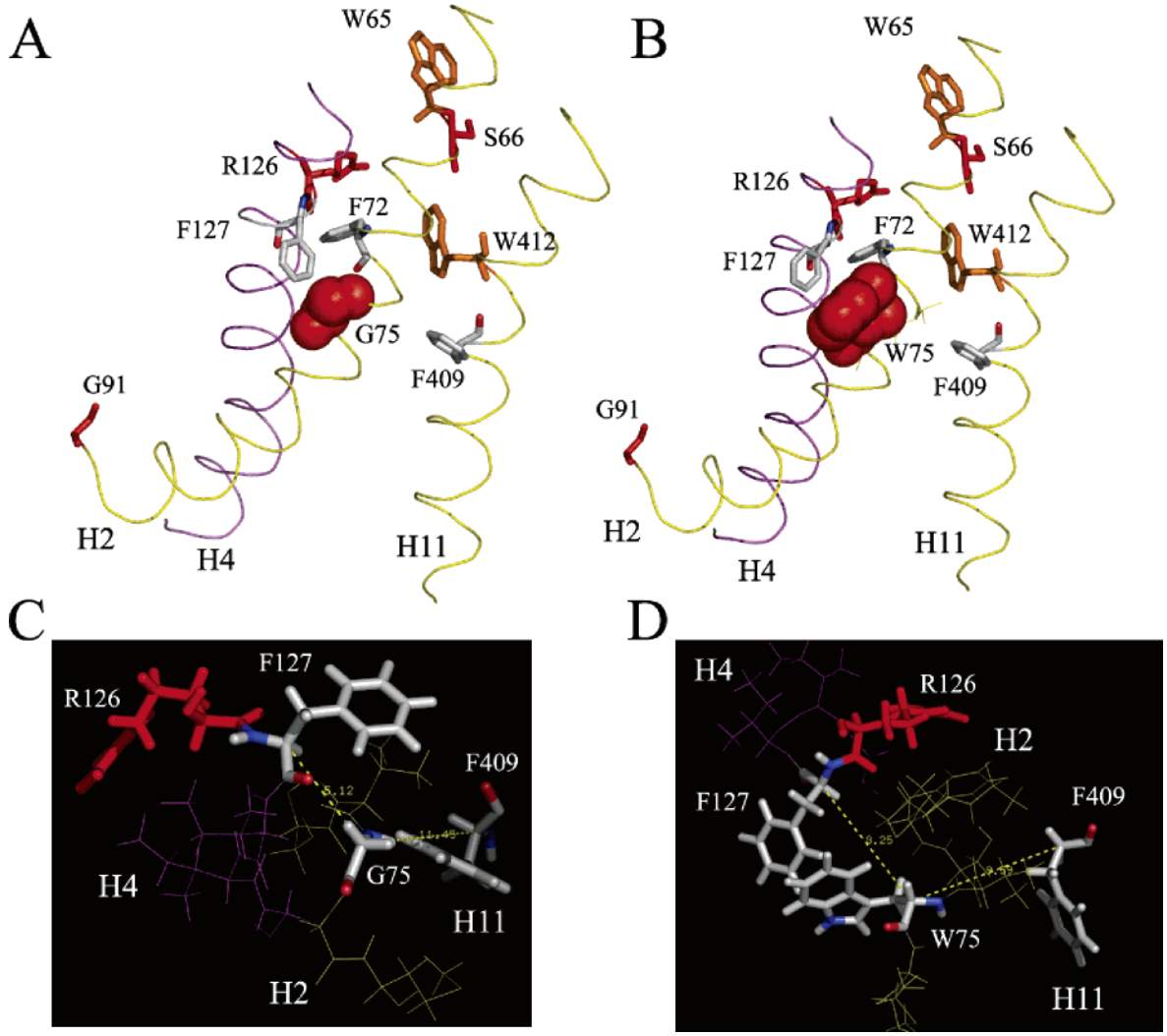

FIGURE 3: Wild-type Glut1 before (A) and after (C) molecular dynamics simulation and the G75W mutant (B and D, respectively). (A) Ribbon and stick representation of transmembrane segments 2, 4, and 11. Residues for which interactions are described are labeled. Red denotes residues that when mutated may induce pathogenicity. (B) Like panel A except for G75W. (C) Greater detail of the region of possible interactions near the fulcrum of transmembrane segments 2 and 4. (D) Like panel C except for G75W. Colors for helical backbones are those corresponding to the nomenclature of Hirai et al. (*32*).

glucose, 2.05 mmol/L; CSF/blood ratio, 0.42), suggestive of impaired GLUT1-mediated glucose transport into the brain. GLUT1 deficiency was confirmed, and a ketogenic diet was initiated. The diet significantly reduced the incidence of seizures and resulted in developmental improvement. The further clinical course was complicated by a variable compliance with the diet that eventually required add-on anticonvulsive medication.

In Vitro Analysis. Glycine 75 is located in the second transmembrane segment of the GLUT1 protein (Figure 1A,B). In 2000, the functional importance of this transmembrane segment (residues L67−V87) was investigated by Olsowski et al. (*1*) by cysteine scanning mutagenesis of the cysteine-less GLUT1. The majority of the cysteine substitution mutants were active transporters except for F72C, G75C, G76C, G79C, and S80C, which exhibited a transport activity percentage lower than 10% of that of the cysteine-less GLUT1. The loss of G75 led to an extremely low 2-deoxyglucose uptake rate of 3% compared with that of the cysteine-less GLUT1 control. In particular, the G75C mutant showed a basal uptake rate of 3 ± 5% (standard deviation). The cluster of three glycine residues (G75, G76, and G79) supported a very tight packing at this particular portion of transmembrane segment 2 with each glycine being absolutely essential for transport activity. As these glycine residues are located on one face of the segment, the authors assumed that they may provide space for a bulky hydrophobic counterpart interacting with another segment or lipid side chain.

Molecular and biochemical GLUT1 analyses in the patient were performed as previously described (*20*). GLUT1-mediated 3-*O*-methyl-D-glucose uptake into patient's erythrocytes showed a reduced apparent K_m value in the patient compared to the intra-assay control (1.4 and 2.0 mmol/L, respectively). V_{max} was reduced to 36% of the intra-assay control [909 and 2500 fmol s^{-1} $(10^6$ RBC$)^{-1}$] (Figure 2). GLUT1-specific immunoblotting of erythrocyte membranes probed with an antibody recognizing the C-terminus of GLUT1 protein (Cymbus Biotechnology, Chandlers Ford, Hants, U.K.) and normalized to band 3 showed normal GLUT1 expression. GLUT1 genomic analyses with PCR and automated sequencing using primers specific to the exon−intron boundaries of the human GLUT1 (*21*) detected a heterozygous single-nucleotide exchange in exon 3 (223G>T) replacing glycine at position 75 with tryptophan. The

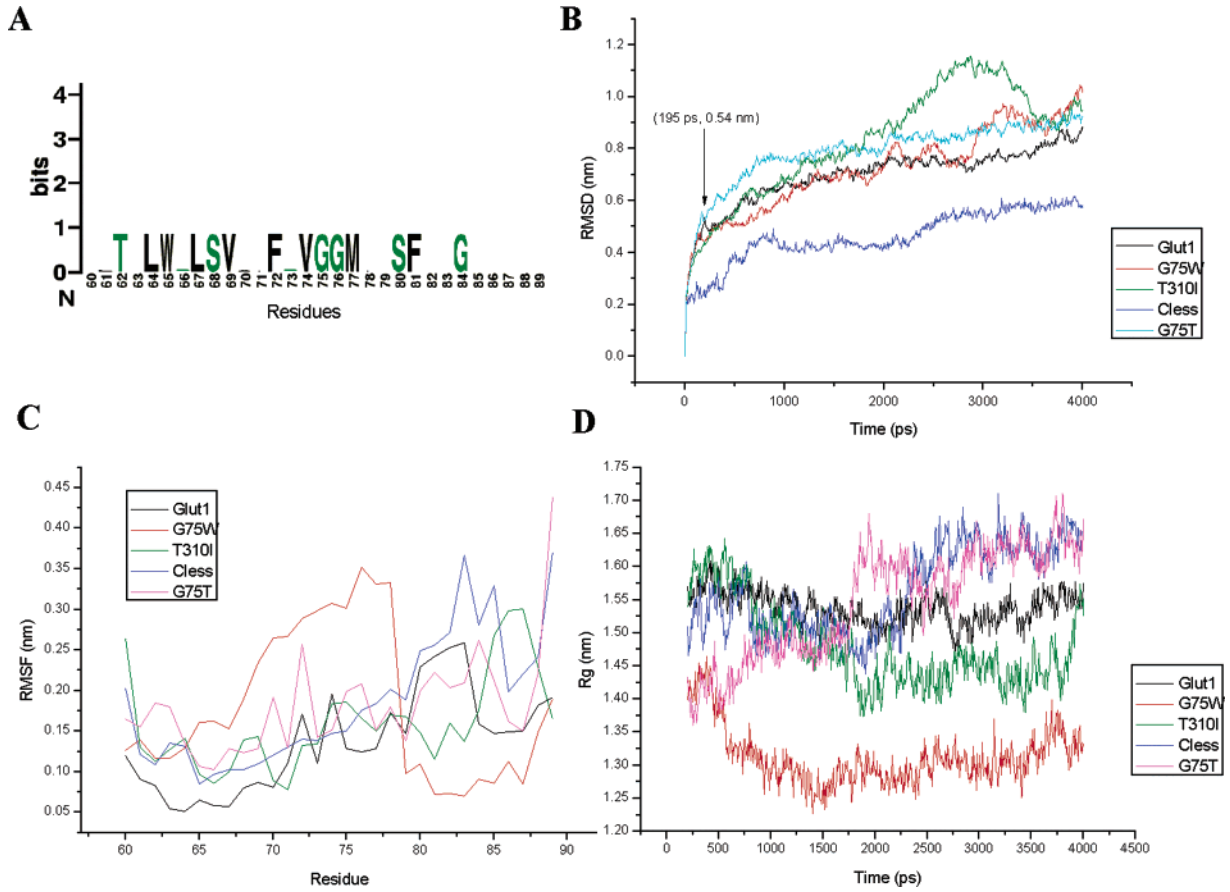

FIGURE 4: (A) Alignment of transmembrane segment 2 in GLUT1−4. Aligment of class 1 GLUTs made with ClustalW (*33*) and plotted with Weblogo (*34*). Green denotes polar amino acids and black hydrophobic ones; conserved residues are enlarged. Panels B−D show the results for GLUT1 isoforms after a 4 ns molecular dynamics simulation in water. (B) Root-mean-square deviation for the proteins. The arrow denotes the equilibration time; the value (0.54) represents the rmsd at that point. (C) Root-mean-square fluctuation for transmembrane segment 2. (D) Gyration radius for transmembrane segment 2.

mutation was confirmed by a band shift polymorphism in the single-stranded DNA conformation polymorphism analysis of exon 3.

In Silico Analysis. Three-dimensional modeling of the G75W mutant was carried out applying molecular dynamics simulations (MDS) based on the GLUT1 model (PDB entry 1SUK). The analysis included as isoforms (a) the wild type, (b) the G75W pathogenic mutant, (c) the T310I pathogenic mutant, (d) the Cys-less GLUT1 (*12*), and (e) the G75T mutant. In the MDS, the GLUT1 was solvated using the water SPC model (*22*) and the OPLS force field (*23*). All runs were at 300 K with a time step of 2 fs, for 4 ns. During the simulation, all bonds were constrained using the LINCS (*24*) algorithm for the protein and SETTLE (*25*) for water. Berendsen's scheme was used for temperature and pressure coupling for both protein and solvent (water). Electrostatic forces were calculated with the PME algorithm (*26*). Initial energy minimization was carried out with the steep descent algorithm (1000 steps) followed by a conjugate gradient to a maximum force of 0.1 kJ mol^{-1} nm^{-1}. All simulations were performed with the GROMACS package, version 3.21 (*27*). For trajectory analysis, the tools included in GROMACS were used; the first 200 ps (equilibration) was neglected (see rmsd plots).

In the in silico GLUT1 model (PDB entry 1SUK), transmembrane segment 2 was adjacent to transmembrane segments 4 and 11, lining the transport channel. Figure 3 shows the relevant areas of GLUT1 before (top panels) and after (bottom panels) the MDS. Residues S66, G75, G91, and R126 in transmembrane segments 2 and 4 influence transport when they are mutated (see Figure 3A). The figure also shows tryptophan residues 65 and 412 that are crucial for transport activity, and a cluster of other aromatic residues that line the putative glucose channel (F72, F127, and F409). Importantly, Figure 3B shows that in the mutant G75W, W75 interacts directly with the F127 residue in transmembrane segment 4, and more weakly with residues F409 and W412 in transmembrane segment 11, thus adding support to the original explanations of Olsowski et al. for the possible reason for the loss of transport activity in the mutant. Comparing the wild-type and G75W isoforms before and after MDS, we found the distance between Cα in G75 (transmembrane segment 2) and Cα in F127 (transmembrane segment 4) was decreased in the wild type (from 5.9 to 5.1 Å, Figure 3C) and increased in the mutant (from 6.2 to 8.2 Å, Figure 3D); presumably, the newly inserted tryptophan residue induced accommodations around its volume. The G75-G76 glycine cluster was found to affect transport (*1*). An alignment for the GLUTs of class 1 (GLUT1−4) revealed (Figure 4A) that hydrophobic residues were conserved in transmembrane segment 2, and also that glycines 75 and 76 were well conserved. The assumption that the tryptophan residue resulting from the G75W mutation could interfere with protein motions was studied by MDS for the wild type and the mutant. The system required ~200 ps for stabilization (rmsd plots, Figure 4B). This interval was considered the

time for equilibration, and data for it were neglected. For the remaining interval, rmsf, gyration radius, and energy were calculated. The simulation showed that the structures of the wild type and the G75W mutant were different; the MDS backbone rmsd fit was 1.072. The rmsf for the residues of transmembrane segment 2 was progressively higher, indicating high mobility for all isoforms except for the mutant G75W, in which the residues at the intracellular end of transmembrane segment 2 had fewer fluctuations (Figure 4C). Compared to those of all other isoforms (wild type, T310I, C-less, and G75W mutants), the gyration radius for transmembrane segment 2 was much smaller for the G75W mutant (Figure 4D). This lower mobility of transmembrane segment 2 had its counterpart in a lower total energy for the G75W mutant during the MDS (data not shown).

DISCUSSION

For decades, the pivotal role of glucose transport in energy metabolism has been a main target for research. Within the family of facilitated glucose transporters (GLUTs), GLUT1 has been most extensively studied. Researchers probed the structure of GLUT1, characterizing transmembrane segments, substrate binding sites, and functional domains (*28*). Individual amino acids of interest were investigated by site-directed mutagenesis and expression of mutants in cell systems. Important insights were gained by these powerful in vitro tools, but it was not before the change of the millennium that specific glucose transporter diseases were recognized as clinical entities and these techniques applied to elucidate pathogenic mechanisms in GLUT1 deficiency syndrome (*29*, *30*). The heterozygous GLUT1 G75W missense mutation within transmembrane segment 2 replaces glycine, a small, neutral amino acid, with tryptophan, a nonionic, polar amino acid. This will effectively disrupt the cluster of glycine residues within this segment and potentially any interaction with other segments or lipid side chains. The report by Olsowski et al. (*1*) provided the first evidence that the cluster of glycine residues (G75, GT76, and G79) was essential for GLUT1 function, and that the G75W mutation in our patient should indeed be pathogenic. This was further supported by the three-dimensional modeling of the mutant described here. The reduced radius of gyration of transmembrane segment 2 (Figure 4D) ought to be considered together with Figure 3, which shows that in the mutant, W75 is in close interaction with F127, and also close to F409, F72, and W412. Potentially aromatic interactions generated by the mutation impart relative immobility to the ensemble of transmembrane segments 2 and 4. The mutation is near the fulcrum of segment 2 to segment 4 where it can stabilize the relative positions of both segments. It is suggestive that in segment 2 the residues up to residue 77 have increased mobility (Figure 4C) while those at the intracellular end are more stabilized; presumably, the mutation resulted in a reorientation of the rest of the segment. The increased stability of this intracellular end of transmembrane segment 2 corresponds well with the decreased gyration radius for this segment (Figure 4D). As glucose transport is associated with conformational changes (*14*), the lower mobility of the mutation site and of the global G75W mutant structure could potentially interfere with glucose transport.

Assessing the impact of this mutation on GLUT1 structure and function required in vivo, in vitro, and in silico analyses. These collaborative efforts eventually identified the mutation as pathogenic, confirming it as the cause of GLUT1 deficiency in this patient. This is particularly important as few patients are identified to date and no genotype−phenotype correlation has yet emerged because of the complexity and novelty of the disease. The ongoing dialogue between clinicians and biochemists on the subject of GLUT1 deficiency syndrome has produced previous interesting results. In 1999, we described a girl carrying a missense mutation in exon 7 that resulted in impaired GLUT1-mediated transport for glucose and dehydroascorbic acid, documenting the multifunctional role of the GLUT1 transporter (*20*). In 2001, we identified a family with three affected members and an autosomal-dominant transmitted heterozygous missense mutation in a highly conserved GRR motif of the GLUT1 transporter and confirmed its pathogenicity by in vitro mutagenesis and kinetic analysis of the mutants in the *Xenopus* oocyte system (*31*). Recently, 10 additional pathogenic mutants have been modeled in silico, again illustrating the potential of combined basic and clinical research (*11*). Such collaborations provide substantial information about crucial amino acid residues, their potential interaction with functional domains, and the impact on the glucose transport pathway in individual patients, thus advancing our understanding of the facilitative GLUT1 transporter in health and disease for the benefit of patients.

ACKNOWLEDGMENT

We are indebted to the treating physicians, the patient, and her family for their help, cooperation, and support. Also, we are particularly grateful to Bärbel Leiendecker, dietician, for providing the ketogenic diet and for editorial assistance with the manuscript.

SUPPORTING INFORMATION AVAILABLE

Figure 1 showing (3A) a quantitative Western blot of GLUT1 at 55 kDa in erythrocyte membranes from patient and a control normalized to band 3 and (3B,C) a fragment containing exon 3 and intron−exon boundaries amplified from genomic DNA. SSCP analysis of the resultant DNA showed an additional band in the patient (3B). Automated DNA sequence identified a G to T transversion (↓) at nucleotide 223 (nucleotide +1 is the A of the ATG translation initiation codon, GenBank entry NM_006516) resulting in the G75W amino acid exchange (3C). Picture 1 showing a 10-year-old girl with GLUT1 deficiency syndrome caused by the G75W mutation in the GLUT1 gene. This material is available free of charge via the Internet at http://pubs.acs.org.

REFERENCES

1. Olsowski, A., Monden, I., Krause, G., and Keller, K. (2000) Cysteine scanning mutagenesis of helices 2 and 7 in GLUT1 identifies an exofacial cleft in both transmembrane segments, *Biochemistry 39*, 2469−74.
2. Klepper, J. (2004) Impaired glucose transport into the brain: The expanding spectrum of glucose transporter type 1 deficiency syndrome, *Curr. Opin. Neurol. 17*, 193−6.
3. Gerhart, D. Z., LeVasseur, R. J., Broderius, M. A., and Drewes, L. R. (1989) Glucose transporter localization in brain using light and electron immunocytochemistry, *J. Neurosci. Res. 22*, 464−72.
4. Mueckler, M., Caruso, C., Baldwin, S. A., Panico, M., Blench, I., Morris, H. R., Allard, W. J., Lienhard, G. E., and Lodish, H. F.

(1985) Sequence and structure of a human glucose transporter, *Science 229*, 941−5.
5. McGowan, K. M., Long, S. D., and Pekala, P. H. (1995) Glucose transporter gene expression: Regulation of transcription and mRNA stability, *Pharmacol. Ther. 66*, 465−505.
6. Hresko, R. C., Kruse, M., Strube, M., and Mueckler, M. (1994) Topology of the glut 1 glucose transporter deduced from glycosylation scanning mutagenesis, *J. Biol. Chem. 269*, 20482−8.
7. Mueckler, M. (1994) Facilitative glucose transporters, *Eur. J. Biochem. 219*, 713−25.
8. Hashiramoto, M., Kadowaki, T., Clark, A. E., Muraoka, A., Momomura, K., Sakura, H., Tobe, K., Akanuma, Y., Yazaki, Y., Holman, G. D., and Kasuga, M. (1992) Site-directed mutagenesis of GLUT1 in helix 7 residue 282 results in perturbation of exofacial ligand binding, *J. Biol. Chem. 267*, 17502−7.
9. Garcia, J. C., Strube, M., Leingang, K., Keller, K., and Mueckler, M. M. (1992) Amino Acid Substitution at Tryptophan 388 and Tryptophan 412 of the HepG2 (Glut1) Glucose Transporter Inhibit Transport Activity and Targeting to the Plasma membrane in *Xenopus* Oocytes, *J. Biol. Chem. 267*, 7770−6.
10. Muraoka, A., Hashiramoto, M., Clark, A. E., Edwards, L. C., Sakura, H., Kadowaki, T., Holman, G. D., and Kasuga, M. (1995) Analysis of the structural features of the C-terminus of GLUT1 that are required for transport catalytic activity, *Biochem. J. 311*, 699−704.
11. Salas-Burgos, A., Iserovich, P., Zuniga, F., Vera, J. C., and Fischbarg, J. (2004) Predicting the three-dimensional structure of the human facilitative glucose transporter glut1 by a novel evolutionary homology strategy: Insights on the molecular mechanism of substrate migration, and binding sites for glucose and inhibitory molecules, *Biophys. J. 87*, 2990−9.
12. Mueckler, M., and Makepeace, C. (1997) Identification of an amino acid residue that lies between the exofacial vestibule and exofacial substrate-binding site of the Glut1 sugar permeation pathway, *J. Biol. Chem. 272*, 30141−6.
13. Widdas, W. F. (1998) The glucose transporter of human erythrocytes: Working hypothesis for its functional mechanism, *Exp. Physiol. 83*, 186−94.
14. Carruthers, A. (1990) Facilitated Diffusion of Glucose, *Physiol. Rev. 70*, 1135−75.
15. Holman, G. D. (1980) An allosteric pore model for sugar transport in human erythrocytes, *Biochim. Biophys. Acta 599*, 202−13.
16. Holman, G. D., Busza, A. L., Pierce, E. J., and Rees, W. D. (1981) Evidence for negative cooperativity in human erythrocyte sugar transport, *Biochim. Biophys. Acta 649*, 503−14.
17. De Vivo, D. C., Trifiletti, R. R., Jacobson, R. I., Ronen, G. M., Behmand, R. A., and Harik, S. I. (1991) Defective glucose transport across the blood-brain barrier as a cause of persistent hypoglycorrhachia, seizures, and developmental delay, *N. Engl. J. Med. 325*, 703−9.
18. De Vivo, D. C., Leary, L., and Wang, D. (2002) Glucose transporter 1 deficiency syndrome and other glycolytic defects, *J. Child Neurol. 17*, 315−25.
19. Klepper, J., and Voit, T. (2002) Facilitated glucose transporter protein type 1 (GLUT1) deficiency syndrome: Impaired glucose transport into brain−A review, *Eur. J. Pediatr. 161*, 295−304.
20. Klepper, J., Wang, D., Fischbarg, J., Vera, J. C., Jarjour, I. T., O'Driscoll, K. R., and De Vivo, D. C. (1999) Defective glucose transport across brain tissue barriers: A newly recognized neurological syndrome, *Neurochem. Res. 24*, 587−94.
21. Fukumoto, H., Seino, S., Imura, H., Seino, Y., and Bell, G. I. (1988) Characterization and expression of human HepG2/erythrocyte glucose-transporter gene, *Diabetes 37*, 657−61.
22. Berendsen, H. J. C., Postma, J. P. M., van Gunsteren, W. F., and Hermans, J. (1981) in *Intermolecular Forces* (Pullman, B., Ed.) pp 331−42, Reidel, Dordrecht, The Netherlands.
23. Jorgensen, W. L., and Tirado-Rives, J. (1988) The OPLS potential functions for proteins. Energy minimizations for crystals of cyclic peptides and crambin, *J. Am. Chem. Soc. 110*, 1657−66.
24. Hess, B., Bekker, H., Berendsen, H. J. C., and Fraaije, J. G. E. M. (1997) LINCS: A Linear Constraint Solver for Molecular Simulations, *J. Comput. Chem. 18*, 1463−72.
25. Miyamoto, S., and Kollman, P. A. (1992) SETTLE: An Analytical Version of the SHAKE and RATTLE Algorithms for Rigid Water Models, *J. Comput. Chem. 13*, 952−62.
26. Darden, T. A., York, D., and Pedersen, L. G. (1993) Particle mesh Ewald: An Nlog(N) methods for Ewald sums in large systems, *J. Chem. Phys. 98*, 1089−92.
27. Lindahl, E., Hess, B., and van der Spoel, D. (2001) GROMACS 3.0: A package for molecular simulation and trajectory analysis, *J. Mol. Model. 7*, 306−17.
28. Uldry, M., and Thorens, B. (2004) The SLC2 family of facilitated hexose and polyol transporters, *Pfluegers Arch. 447*, 480−9.
29. Brown, G. K. (2000) Glucose transporters: Structure, function and consequences of deficiency, *J. Inherit. Metab. Dis. 23*, 237−46.
30. De Vivo, D. C., Wang, D., Pascual, J. M., and Ho, Y. Y. (2002) Glucose transporter protein syndromes, *Int. Rev. Neurobiol. 51*, 259−88.
31. Klepper, J., Monden, I., Guertsen, E., Voit, T., Willemsen, M., and Keller, K. (2001) Functional consequences of the autosomal dominant G272A mutation in the human GLUT1 gene, *FEBS Lett. 498*, 104−9.
32. Hirai, T., Heymann, J. A., Maloney, P. C., and Subramaniam, S. (2003) Structural model for 12-helix transporters belonging to the major facilitator superfamily, *J. Bacteriol. 185*, 1712−8.
33. Thompson, J. D., Higgins, D. G., and Gibson, T. J. (1994) CLUSTAL W: Improving the sensitivity of progressive multiple sequence alignment through sequence weighting, position-specific gap penalties and weight matrix choice, *Nucleic Acids Res. 22*, 4673−80.
34. Crooks, G. E., Hon, G., Chandonia, J. M., and Brenner, S. E. (2004) WebLogo: A sequence logo generator, *Genome Res. 14*, 1188−90.

BI051079T